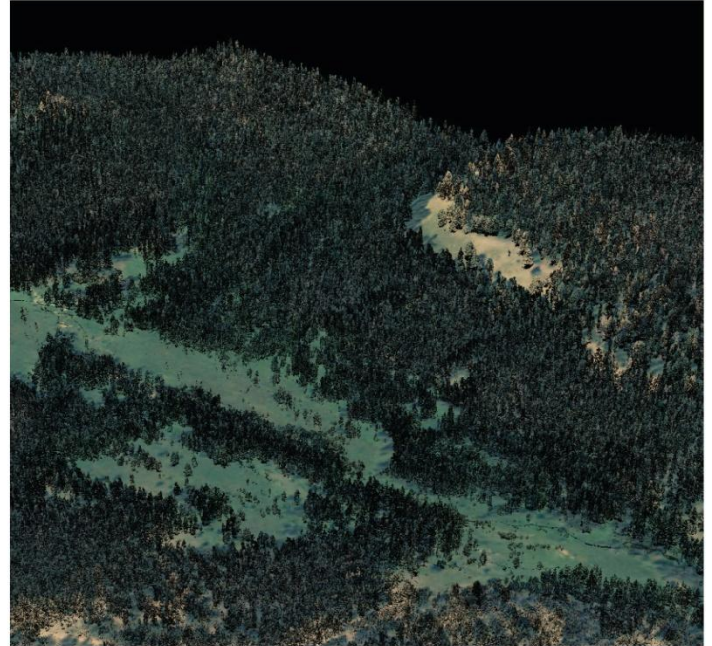
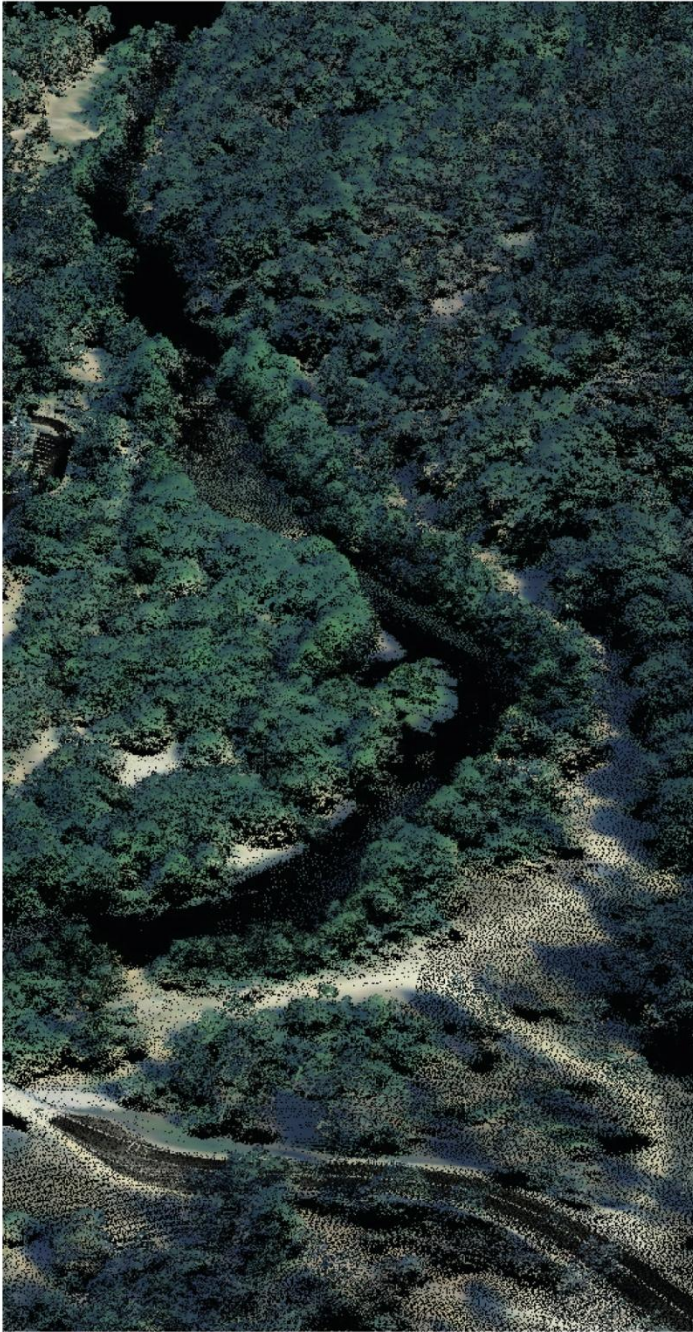


LIDAR REMOTE SENSING & ORTHOPHOTOGRAPHS

STANLEY STUDY AREA • CHALLIS NATIONAL FOREST

(REVISION 1 - 1/28/11)



UNIVERSITY OF IDAHO
DEPT OF GEOGRAPHY

JEFF HICKE & BEN BRIGHT
Univ of Idaho, McClure Hall 203 - Moscow, ID 83844

 WATERSHED SCIENCES • 517 SW 2nd Street, Suite 400 - Corvallis, OR 97333

LIDAR REMOTE SENSING DATA COLLECTION

STANLEY, IDAHO

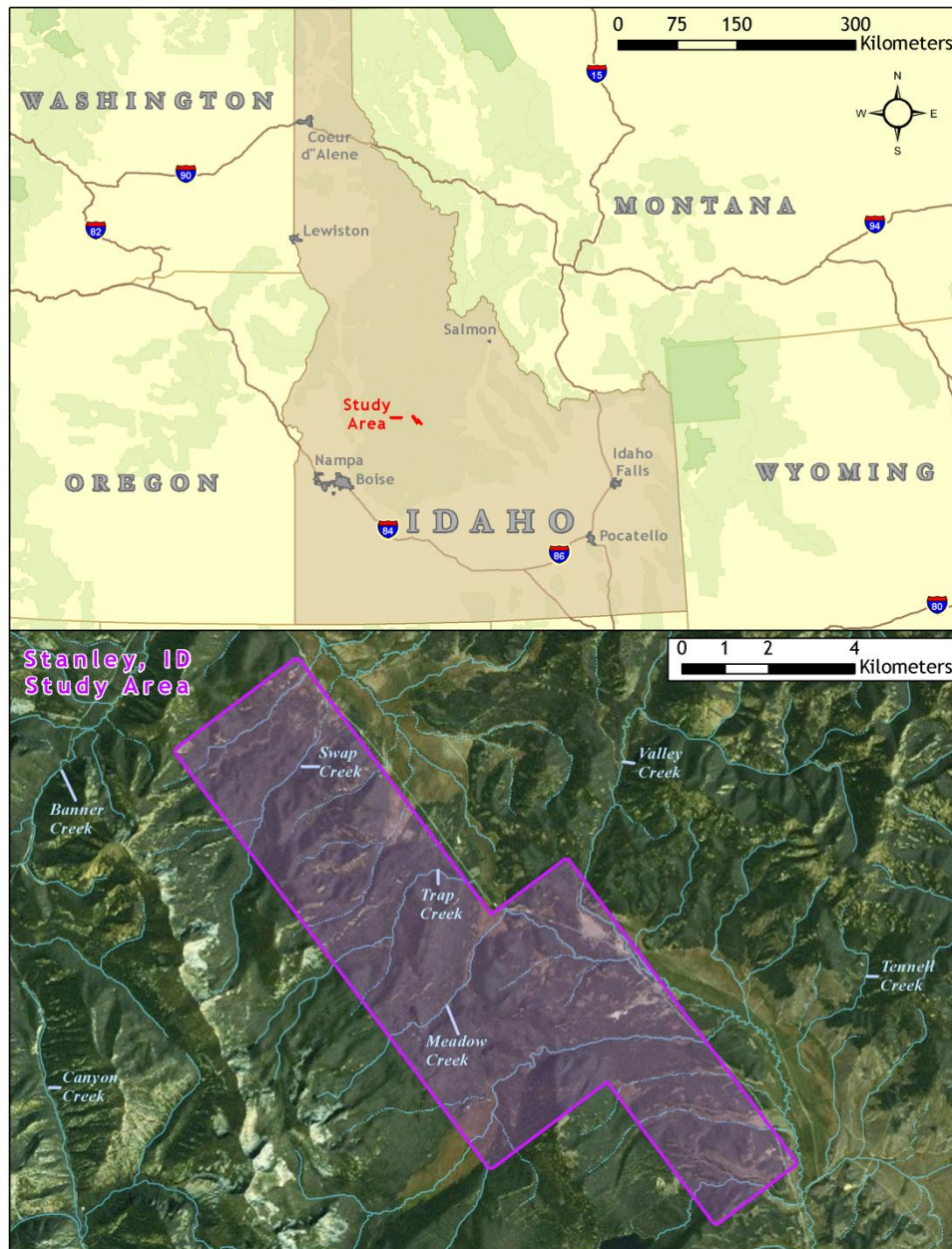
TABLE OF CONTENTS

1. Overview	1
2. Acquisition	2
2.1 Airborne Survey - Instrumentation and Methods.....	2
2.2 Ground Survey - Instrumentation and Methods	3
2.2.1 Instrumentation.....	3
2.2.2 Monumentation	3
2.2.3 Methodology	4
3. LiDAR Data Processing.....	7
3.1 Applications and Work Flow Overview.....	7
3.2 Aircraft Kinematic GPS and IMU Data.....	8
3.3 Laser Point Processing	8
3.4 Orthophotograph Processing	9
4. LiDAR Accuracy Assessment	9
4.1 Laser Noise and Relative Accuracy	9
4.2 Absolute Accuracy	11
5. Photo Accuracy Assessment	11
6. Study Area Results	13
6.1 Data Summary	13
6.2 Data Density/Resolution	13
6.3 Relative Accuracy Calibration Results	17
6.4 Absolute Accuracy	18
6.5 Orthophotograph Accuracy	19
7. Projection/Datum and Units	22
8. Deliverables.....	22
9. Selected Images	23
10. Glossary	28
10. Citations.....	29
Appendix A	30

1. Overview

Watershed Sciences, Inc. (WS) collected Light Detection and Ranging (LiDAR) data of the Stanley study area in Idaho on August 4th and 5th, 2010 and 4 band Orthophotographic imagery on August 13th, 2010. This report documents the data acquisition, processing methods, accuracy assessment, and deliverables for the 14,811 study area. The area was expanded to include a 100 meter buffer to ensure complete coverage and adequate point densities around survey area boundaries, resulting in 15,894 acres of delivered LiDAR data (Figure 1). This completes the Stanley data collection delivery.

Figure 1. Stanley study area



2. Acquisition

2.1 Airborne Survey - Instrumentation and Methods

The LiDAR survey utilized dual-mounted Leica ALS50 Phase II sensors in a Cessna Caravan 208B. The Leica systems were set to acquire $\geq 83,000$ laser pulses per second (i.e., 83 kHz pulse rate) and flown at 900 meters above ground level (AGL), capturing a scan angle of $\pm 13^\circ$ from nadir. These settings are developed to yield points with an average native pulse density of ≥ 8 pulses per square meter over terrestrial surfaces. It is not uncommon for some types of surfaces (e.g. dense vegetation or water) to return fewer pulses than the laser originally emitted. These discrepancies between 'native' and 'delivered' density will vary depending on terrain, land cover and the prevalence of water bodies.



The Cessna Caravan is a stable platform, ideal

for flying slow and low for high density projects. The Leica ALS50 sensor head installed in the Caravan is shown on the left.

All areas were surveyed with an opposing flight line side-lap of $\geq 50\%$ ($\geq 100\%$ overlap) to reduce laser shadowing and increase surface laser painting. The Leica laser systems allow up to four range measurements (returns) per pulse, and all discernable laser returns were processed for the output dataset.

To accurately solve for laser point position (geographic coordinates x, y, z), the positional coordinates of the airborne sensor and the attitude of the aircraft were recorded continuously throughout the LiDAR data collection mission. Aircraft position was measured twice per second (2 Hz) by an onboard differential GPS unit. Aircraft attitude was measured 200 times per second (200 Hz) as pitch, roll and yaw (heading) from an onboard inertial measurement unit (IMU). To allow for post-processing correction and calibration, aircraft/sensor position and attitude data are indexed by GPS time.

The aerial imagery was collected using a Vexcel UltraCam D large format aerial mapping camera capable of simultaneous capture of red, green, blue, and NIR bands. For the Stanley study area, images were collected with 60% along track overlap and 30% sidelap between frames. The acquisition flight parameters were designed to yield native ground pixel resolution of 20 cm.

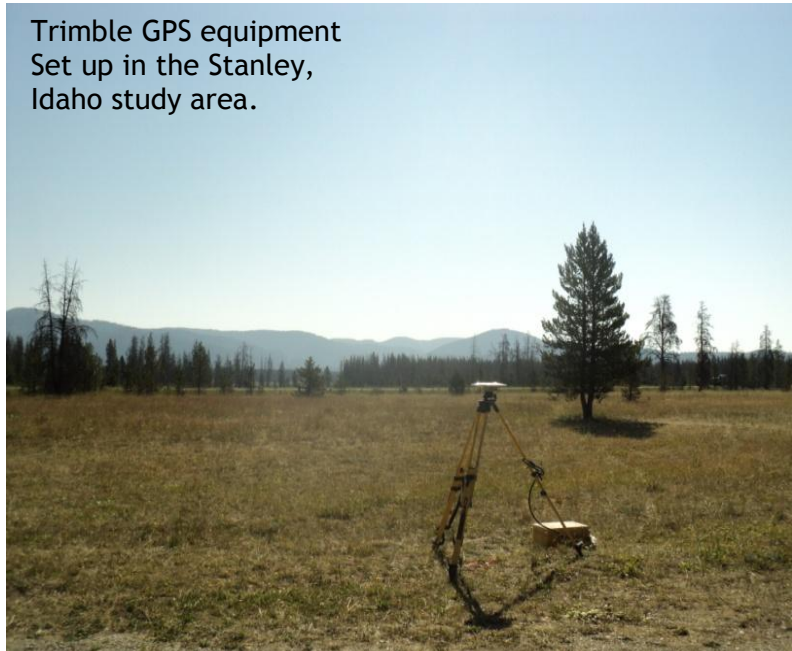
LiDAR Data Acquisition and Processing: Stanley, Idaho

Prepared by Watershed Sciences, Inc.

2.2 Ground Survey - Instrumentation and Methods

During the LiDAR survey, static (1 Hz recording frequency) ground surveys were conducted over set monuments. Monument coordinates for the study area are provided in **Table 1** and shown in **Figure 2**. After the airborne survey, the static GPS data are processed using triangulation with Continuously Operating Reference Station (CORS) and checked using the Online Positioning User Service (OPUS¹) to quantify daily variance. Multiple sessions are processed over the same monument to confirm antenna height measurements and reported position accuracy.

Indexed by time, these GPS data are used to correct the continuous onboard measurements of aircraft position recorded throughout the mission. Control monuments were located within 13 nautical miles of the survey area.



2.2.1 Instrumentation

For this delivery area, a Trimble GPS receiver model R7 with Zephyr Geodetic antenna with ground plane was deployed for all static control. A Trimble model R8 GNSS unit was used for collecting check points using real time kinematic (RTK) survey techniques. For RTK data, the collector begins recording after remaining stationary for 5 seconds then calculating the pseudo range position from at least three epochs with the relative error under 1.5cm horizontal and 2cm vertical. All GPS measurements are made with dual frequency L1-L2 receivers with carrier-phase correction.

2.2.2 Monumentation



Watershed Sciences established two monuments within the study area (**Table 1**). The Watershed Sciences' monumentation was done with 5/8" x 30" rebar topped with a plastic cap marked with the project ID and technicians initials.

¹ Online Positioning User Service (OPUS) is run by the National Geodetic Survey to process corrected monument positions.

Table 1. Base Station Survey Control coordinates for the Stanley study area.

Base Station ID	Datum: NAD83 (CORS96)		GRS80
	Latitude	Longitude	Ellipsoid Z (meters)
STAN_LW1	44° 17' 49.0019	115° 03' 00.1444	1992.117
STAN_LW3	44° 21' 35.3673	115° 08' 21.2812	2010.308

2.2.3 Methodology

Each aircraft is assigned a ground crew member equipped with two Trimble R7 receivers and an R8 receiver. The ground crew vehicles contain standard field survey supplies and equipment including safety materials. All control monuments are observed for a minimum of two survey sessions lasting no fewer than 6 hours. At the beginning of every session the tripod and antenna are reset, resulting in two independent instrument heights and data files. Data is collected at a rate of 1Hz using a 10 degree mask on the antenna.

The ground crew uploads the GPS data to our FTP site on a daily basis to be returned to the office for Professional Land Surveyor (PLS) oversight, QA/QC review and processing. OPUS processing triangulates the monument position using 3 CORS stations resulting in a fully adjusted position. After multiple days of data have been collected at each monument, accuracy and error ellipses are calculated from the OPUS reports. This information leads to a rating of the monument based on FGDC-STD-007.2-1998² Part 2 table 2.1 at the 95% confidence level. When a statistical stable position is found CORPSCON³ 6.0.1 software is used to convert the UTM positions to geodetic positions. This geodetic position is used for processing the LiDAR data.

RTK and aircraft mounted GPS measurements are made during periods with PDOP⁴ less than or equal to 3.0 and with at least 6 satellites in view of both a stationary reference receiver and



Field technician gathering RTK data.

² Federal Geographic Data Committee Draft Geospatial Positioning Accuracy Standards

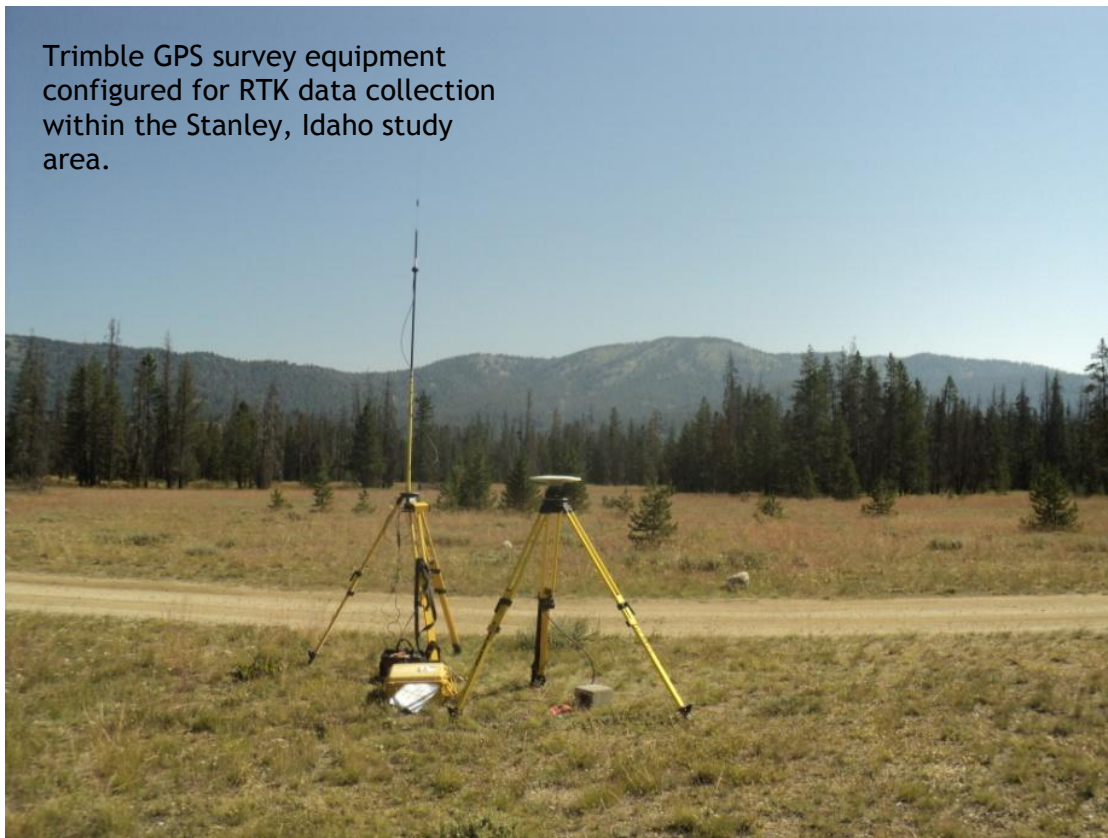
³ U.S. Army Corps of Engineers , Engineer Research and Development Center Topographic Engineering Center software

⁴PDOP: Point Dilution of Precision is a measure of satellite geometry smaller the number the better the geometry between the point and the satellites.

LiDAR Data Acquisition and Processing: Stanley, Idaho

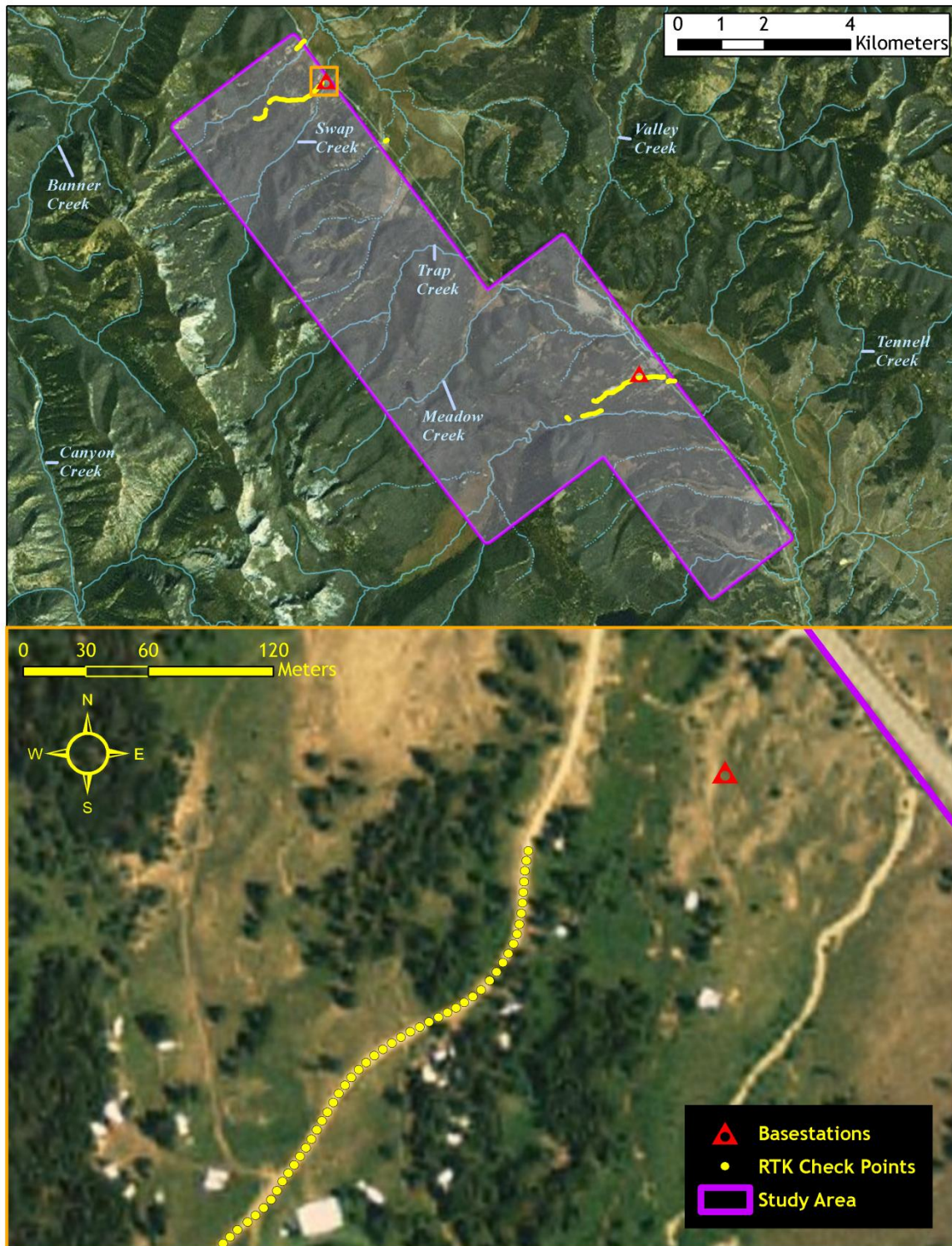
the roving receiver. Static GPS data collected in a continuous session averaging the high PDOP into the final solution, the same way CORS stations operate. RTK positions are collected on 20% of the flight lines and on bare earth locations such as paved, gravel or stable dirt roads, and other locations where the ground is clearly visible (and is likely to remain visible) from the sky during the data acquisition and RTK measurement period(s).

In order to facilitate comparisons with LiDAR measurements, RTK measurements are not taken on highly reflective surfaces such as center line stripes or lane markings on roads. RTK points were taken no closer than one meter to any nearby terrain breaks such as road edges or drop offs.



Trimble GPS survey equipment configured for RTK data collection within the Stanley, Idaho study area.

Figure 2. RTK check point and control monument locations used in the Stanley study area.



3. LiDAR Data Processing

3.1 Applications and Work Flow Overview

1. Resolved kinematic corrections for aircraft position data using kinematic aircraft GPS and static ground GPS data.
Software: Waypoint GPS v.8.10, Trimble Geomatics Office v.1.62
2. Developed a smoothed best estimate of trajectory (SBET) file that blends post-processed aircraft position with attitude data. Sensor head position and attitude were calculated throughout the survey. The SBET data were used extensively for laser point processing.
Software: IPAS v.1.35
3. Calculated laser point position by associating SBET position to each laser point return time, scan angle, intensity, etc. Created raw laser point cloud data for the entire survey in *.las (ASPRS v. 1.2) format.
Software: ALS Post Processing Software v.2.70
4. Imported raw laser points into manageable blocks (less than 500 MB) to perform manual relative accuracy calibration and filter for pits/birds. Ground points were then classified for individual flight lines (to be used for relative accuracy testing and calibration).
Software: TerraScan v.10.009
5. Using ground classified points per each flight line, the relative accuracy was tested. Automated line-to-line calibrations were then performed for system attitude parameters (pitch, roll, heading), mirror flex (scale) and GPS/IMU drift. Calibrations were performed on ground classified points from paired flight lines. Every flight line was used for relative accuracy calibration.
Software: TerraMatch v.10.006
6. Position and attitude data were imported. Resulting data were classified as ground and non-ground points. Statistical absolute accuracy was assessed via direct comparisons of ground classified points to ground RTK survey data. Data were then converted to orthometric elevations (NAVD88) by applying a Geoid03 correction.
Software: TerraScan v.10.009, TerraModeler v.10.004
7. Bare Earth models were created as a triangulated surface and exported as ArcInfo ASCII grids at a 1-meter pixel resolution.
Software: TerraScan v.10.009, ArcMap v. 9.3.1, TerraModeler v.10.004

3.2 Aircraft Kinematic GPS and IMU Data

LiDAR survey datasets were referenced to the 1 Hz static ground GPS data collected over pre-surveyed monuments with known coordinates. While surveying, the aircraft collected 2 Hz kinematic GPS data, and the onboard inertial measurement unit (IMU) collected 200 Hz aircraft attitude data. Waypoint GPS v.8.10 was used to process the kinematic corrections for the aircraft. The static and kinematic GPS data were then post-processed after the survey to obtain an accurate GPS solution and aircraft positions. IPAS v.1.35 was used to develop a trajectory file that includes corrected aircraft position and attitude information. The trajectory data for the entire flight survey session were incorporated into a final smoothed best estimated trajectory (SBET) file that contains accurate and continuous aircraft positions and attitudes.

3.3 Laser Point Processing

Laser point coordinates were computed using the IPAS and ALS Post Processor software suites based on independent data from the LiDAR system (pulse time, scan angle), and aircraft trajectory data (SBET). Laser point returns (first through fourth) were assigned an associated (x, y, z) coordinate along with unique intensity values (0-255). The data were output into large LAS v. 1.2 files with each point maintaining the corresponding scan angle, return number (echo), intensity, and x, y, z (easting, northing, and elevation) information.

These initial laser point files were too large for subsequent processing. To facilitate laser point processing, bins (polygons) were created to divide the dataset into manageable sizes (< 500 MB). Flightlines and LiDAR data were then reviewed to ensure complete coverage of the survey area and positional accuracy of the laser points.

Laser point data were imported into processing bins in TerraScan, and manual calibration was performed to assess the system offsets for pitch, roll, heading and scale (mirror flex). Using a geometric relationship developed by Watershed Sciences, each of these offsets was resolved and corrected if necessary.

LiDAR points were then filtered for noise, pits (artificial low points), and birds (true birds as well as erroneously high points) by screening for absolute elevation limits, isolated points and height above ground. Each bin was then manually inspected for remaining pits and birds and spurious points were removed. In a bin containing approximately 7.5-9.0 million points, an average of 50-100 points are typically found to be artificially low or high. Common sources of non-terrestrial returns are clouds, birds, vapor, haze, decks, brush piles, etc.

Internal calibration was refined using TerraMatch. Points from overlapping lines were tested for internal consistency and final adjustments were made for system misalignments (i.e., pitch, roll, heading offsets and scale). Automated sensor attitude and scale corrections yielded 3-5 cm improvements in the relative accuracy. Once system misalignments were corrected, vertical GPS drift was then resolved and removed per flight line, yielding a slight improvement (<1 cm) in relative accuracy.

The TerraScan software suite is designed specifically for classifying near-ground points (Soininen, 2004). The processing sequence began by ‘removing’ all points that were not ‘near’ the earth based on geometric constraints used to evaluate multi-return points. The resulting bare earth (ground) model was visually inspected and additional ground point modeling was performed in site-specific areas to improve ground detail. This manual editing of ground often occurs in areas with known ground modeling deficiencies, such as: bedrock outcrops, cliffs, deeply incised stream banks, and dense vegetation. In some cases, automated ground point classification erroneously included known vegetation (i.e., understory, low/dense shrubs, etc.). These points were manually reclassified as default. Ground surface rasters were then developed from triangulated irregular networks (TINs) of ground points.

3.4 Orthophotograph Processing

Image radiometric values were calibrated to specific gain and exposure settings associated with each capture and saved in tiff format. Photo position and orientation was then calculated by assigning aircraft position and attitude information to each image by associating the time of image capture with trajectory file (SBET). Photos were then orthorectified using control points derived from the LiDAR intensity image using LPS.

The rectified images were mosaicked together in a three step process using Orthovista. Firstly color correction was applied to each image using global tilting adjustments designed to homogenize overlapping regions. Secondly, discrepancies between images were minimized by an automated seam generation process. The most nadir portion of each image was selected and seams were drawn around landscape features. The high resolution orthophotos were delineated into a manageable size (750 x 750 m) appropriate to the pixel resolution and requested spatial reference.

4. LiDAR Accuracy Assessment

4.1 Laser Noise and Relative Accuracy

Laser Noise

For any given target, laser noise is the breadth of the data cloud per laser return (i.e., last, first, etc.). Lower intensity surfaces (roads, rooftops, still/calm water) experience higher laser noise. The laser noise range for this survey was approximately 0.02 meters.

Relative Accuracy

Relative accuracy refers to the internal consistency of the data set - the ability to place a laser point in the same location over multiple flight lines, GPS conditions, and aircraft attitudes. Affected by system attitude offsets, scale, and GPS/IMU drift, internal consistency is measured as the divergence between points from different flight lines within an overlapping area. Divergence is most apparent when flight lines are opposing. When the LiDAR system is well calibrated, the line-to-line divergence is low (<10 cm). See Appendix A for further information on sources of error and operational measures that can be taken to improve relative accuracy.

Relative Accuracy Calibration Methodology

LiDAR Data Acquisition and Processing: Stanley, Idaho

Prepared by Watershed Sciences, Inc.

1. Manual System Calibration: Calibration procedures for each mission require solving geometric relationships that relate measured swath-to-swath deviations to misalignments of system attitude parameters. Corrected scale, pitch, roll and heading offsets were calculated and applied to resolve misalignments. The raw divergence between lines was computed after the manual calibration was completed and reported for each survey area.
2. Automated Attitude Calibration: All data were tested and calibrated using TerraMatch automated sampling routines. Ground points were classified for each individual flight line and used for line-to-line testing. System misalignment offsets (pitch, roll and heading) and scale were solved for each individual mission and applied to respective mission datasets. The data from each mission were then blended when imported together to form the entire area of interest.
3. Automated Z Calibration: Ground points per line were used to calculate the vertical divergence between lines caused by vertical GPS drift. Automated Z calibration was the final step employed for relative accuracy calibration.

4.2 Absolute Accuracy

Laser point absolute accuracy is largely a function of laser noise and relative accuracy. To minimize these contributions to absolute error, we first performed a number of noise filtering and calibration procedures prior to evaluating absolute accuracy. Our LiDAR quality assurance process uses the data from the real-time kinematic (RTK) ground survey conducted in the survey area. For this project a total of **880 RTK GPS** measurements were collected on hard surfaces distributed among multiple flight swaths. To assess absolute accuracy the location coordinates of these known RTK ground survey point were compared to those calculated for the closest laser points.

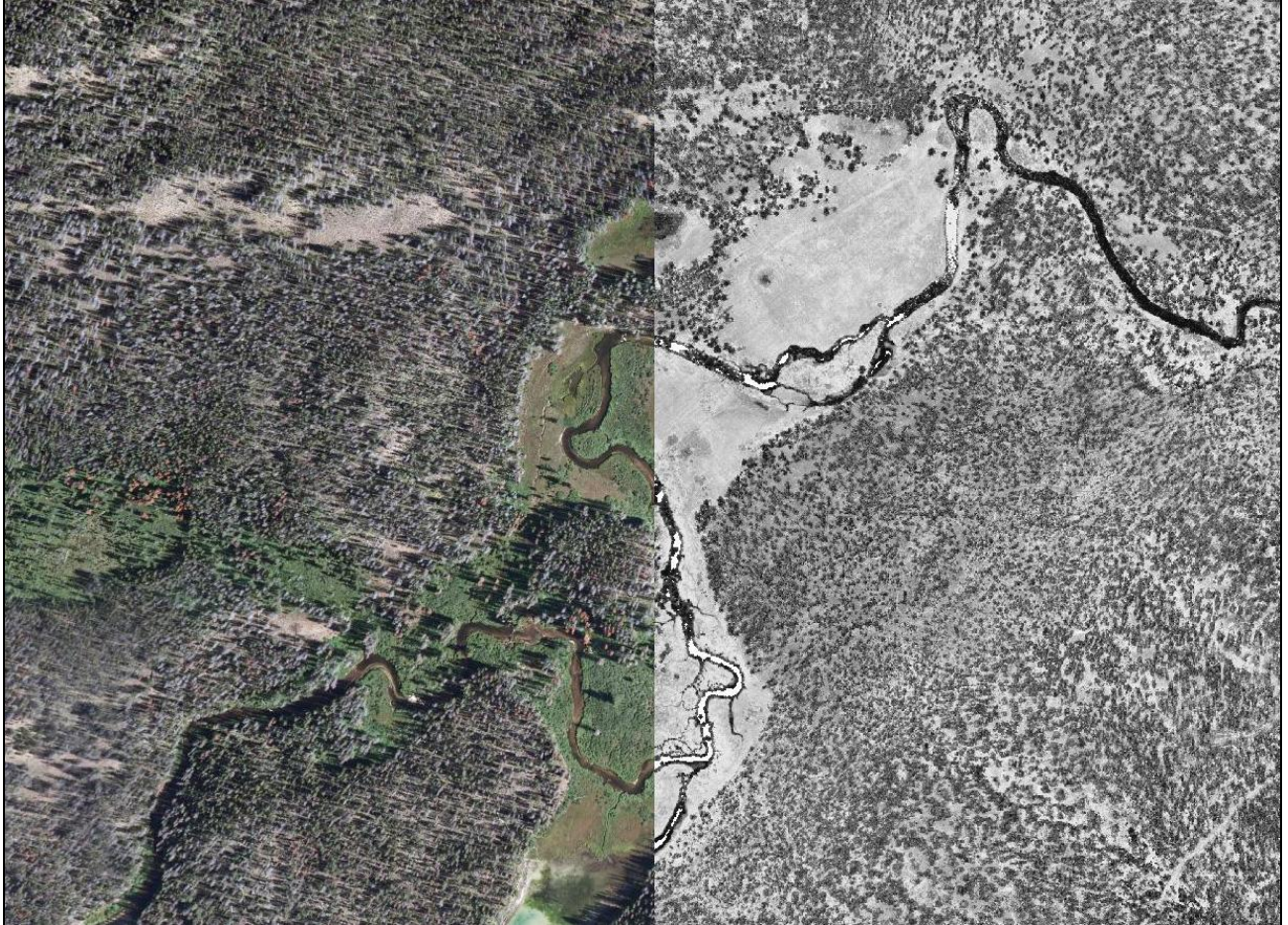
The vertical accuracy of the LiDAR data is described as the mean and standard deviation (sigma $\sim\sigma$) of divergence of LiDAR point coordinates from RTK ground survey point coordinates. To provide a sense of the model predictive power of the dataset, the root mean square error (RMSE) for vertical accuracy is also provided. These statistics assume the error distributions for x, y, and z are normally distributed, thus we also consider the skew and kurtosis of distributions when evaluating error statistics.

To calibrate laser accuracy for the Stanley dataset 880 RTK points were collected on fixed, hard-packed road surfaces within the survey area. Statements of statistical accuracy apply to fixed terrestrial surfaces only and may not be applied to areas of dense vegetation or steep terrain (See Appendix A).

5. Photo Accuracy Assessment

To assess spatial accuracy of the orthophotos they are compared against control points from the LiDAR intensity images. The control points were collected and measured on surface features identifiable in both images. These control points along with auto tie points (image to image references) were used to perform aerial triangulation (AT) adjustments that orthorectify the photos by correctly placing them relative to ground surfaces. The accuracy of the final mosaic, expressed as root mean square error (RMSE), was calculated in relation to the LiDAR-derived control points. **Figure 3** shows the co-registration between orthorectified photographs and LiDAR intensity images.

Figure 3. Example of co-registration of color images with LiDAR intensity images.



6. Study Area Results

Summary statistics for point resolution and accuracy (relative and absolute) of the LiDAR data collected in the Stanley study area are presented below in terms of central tendency, variation around the mean, and the spatial distribution of the data (for point resolution by tile).

6.1 Data Summary

Table 2. LiDAR Resolution and Accuracy - Specifications and Achieved Values

	Targeted	Achieved
Resolution:	≥ 8 points/m ²	8.68 points/m ²
Vertical Accuracy (1 σ):	<15 cm	3.28 cm

6.2 Data Density/Resolution

The average first-return density of delivered dataset is 8.68 points per square meter (Table 2). The initial dataset, acquired to be ≥ 8 points per square meter, was filtered as described previously to remove spurious or inaccurate points. Additionally, some types of surfaces (i.e., dense vegetation, breaks in terrain, water, steep slopes) may return fewer pulses (delivered density) than the laser originally emitted (native density).

Ground classifications were derived from automated ground surface modeling and manual, supervised classifications where it was determined that the automated model had failed. Ground return densities will be lower in areas of dense vegetation, water, or buildings.

Cumulative LiDAR data resolution for the Stanley study area:

- Average Point (First Return) Density = 8.68 points/m²
- Average Ground Point Density = 2.55 points/m²

Figure 4. Density distribution for first return laser points

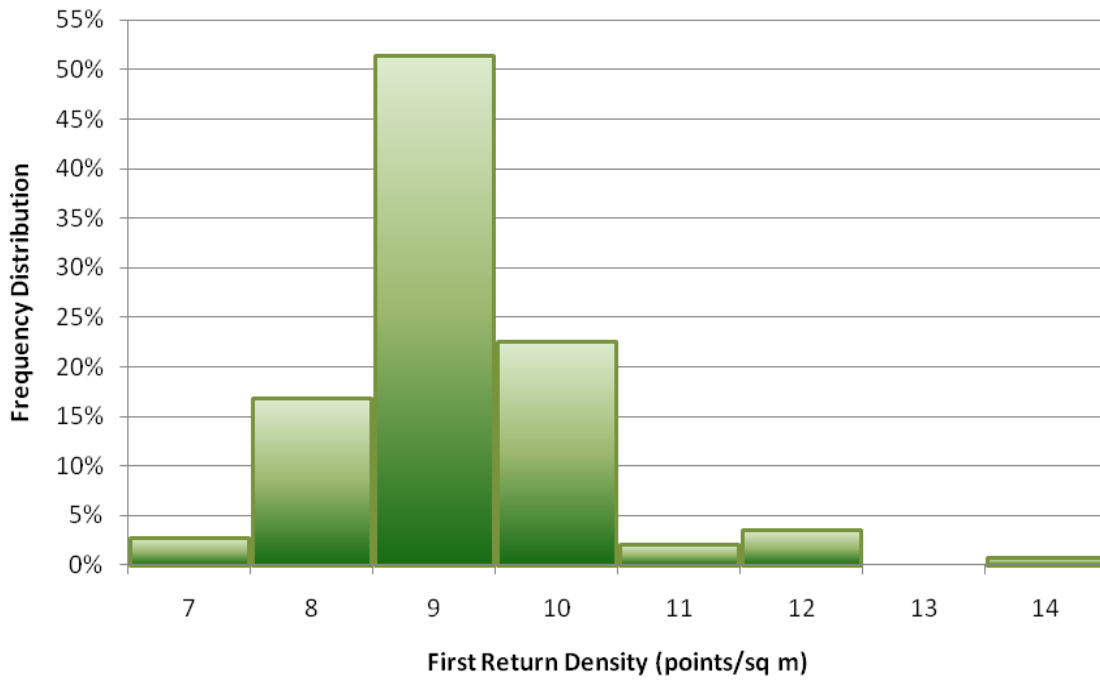


Figure 5. Density distribution for ground classified laser points

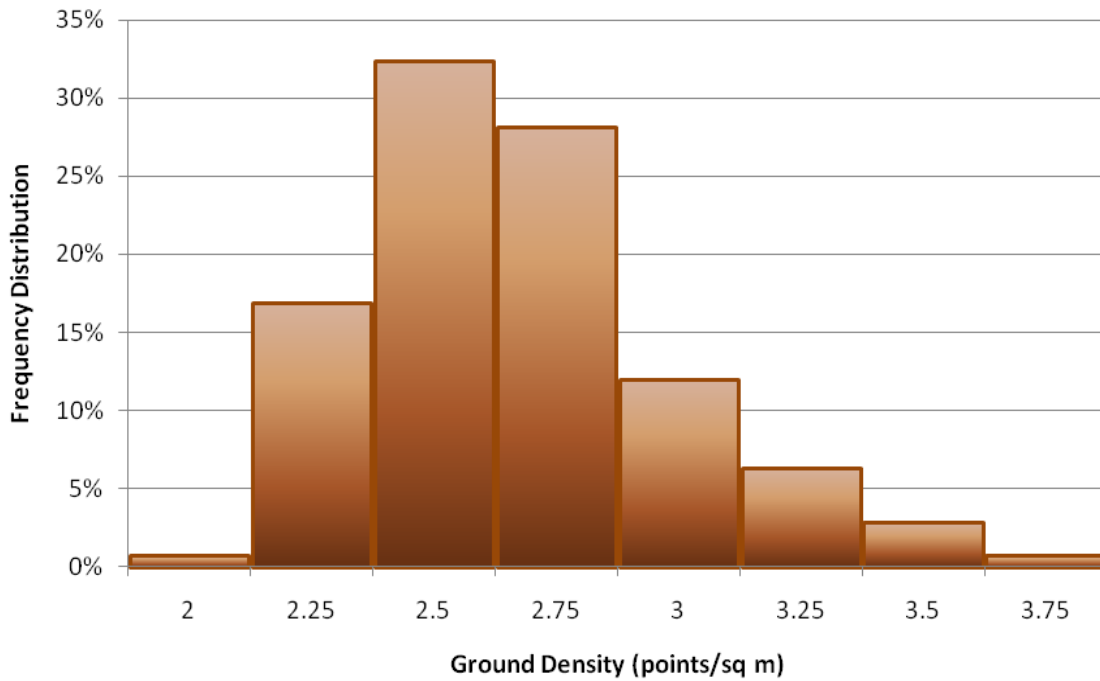


Figure 6. Density distribution map for first return points by processing tile

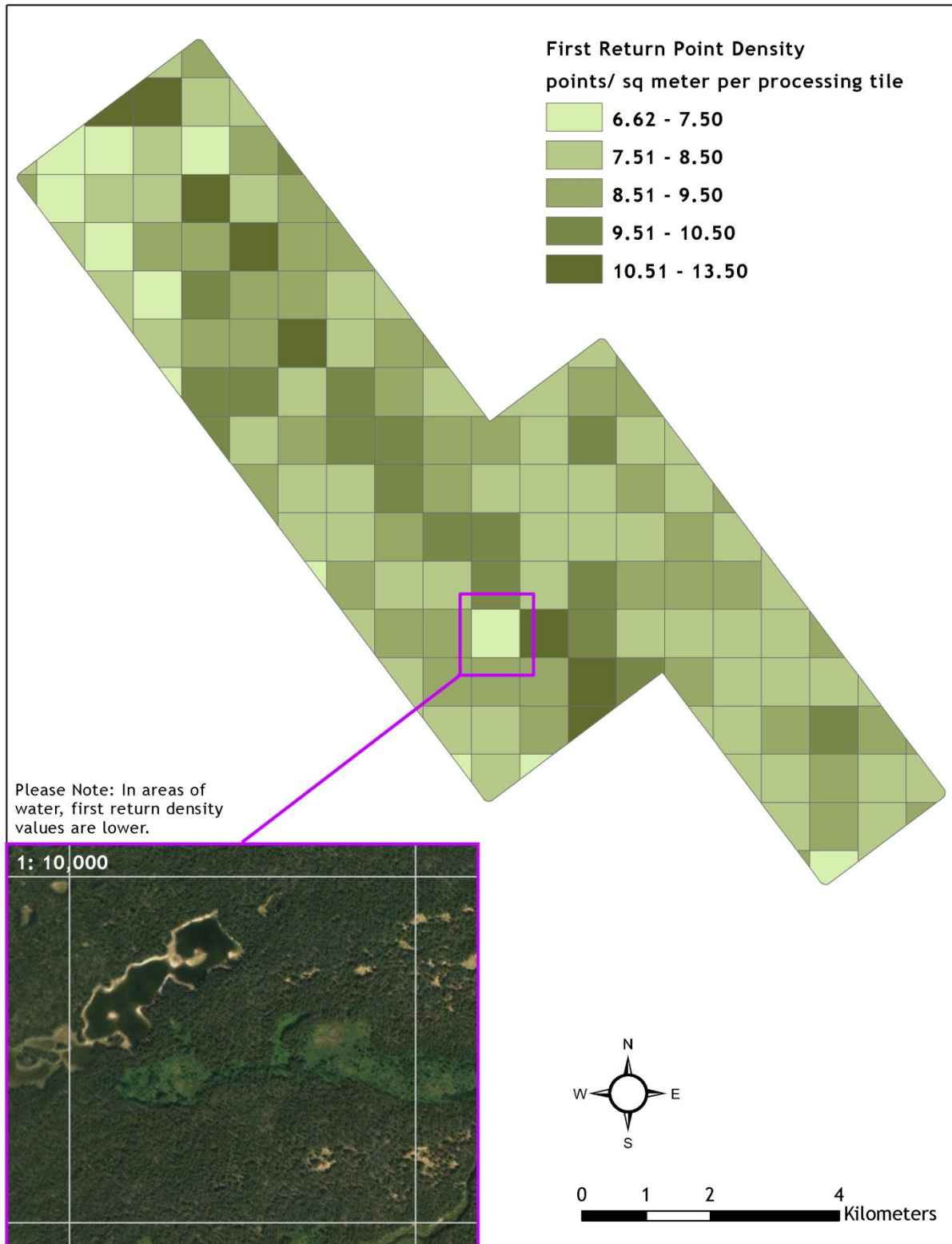
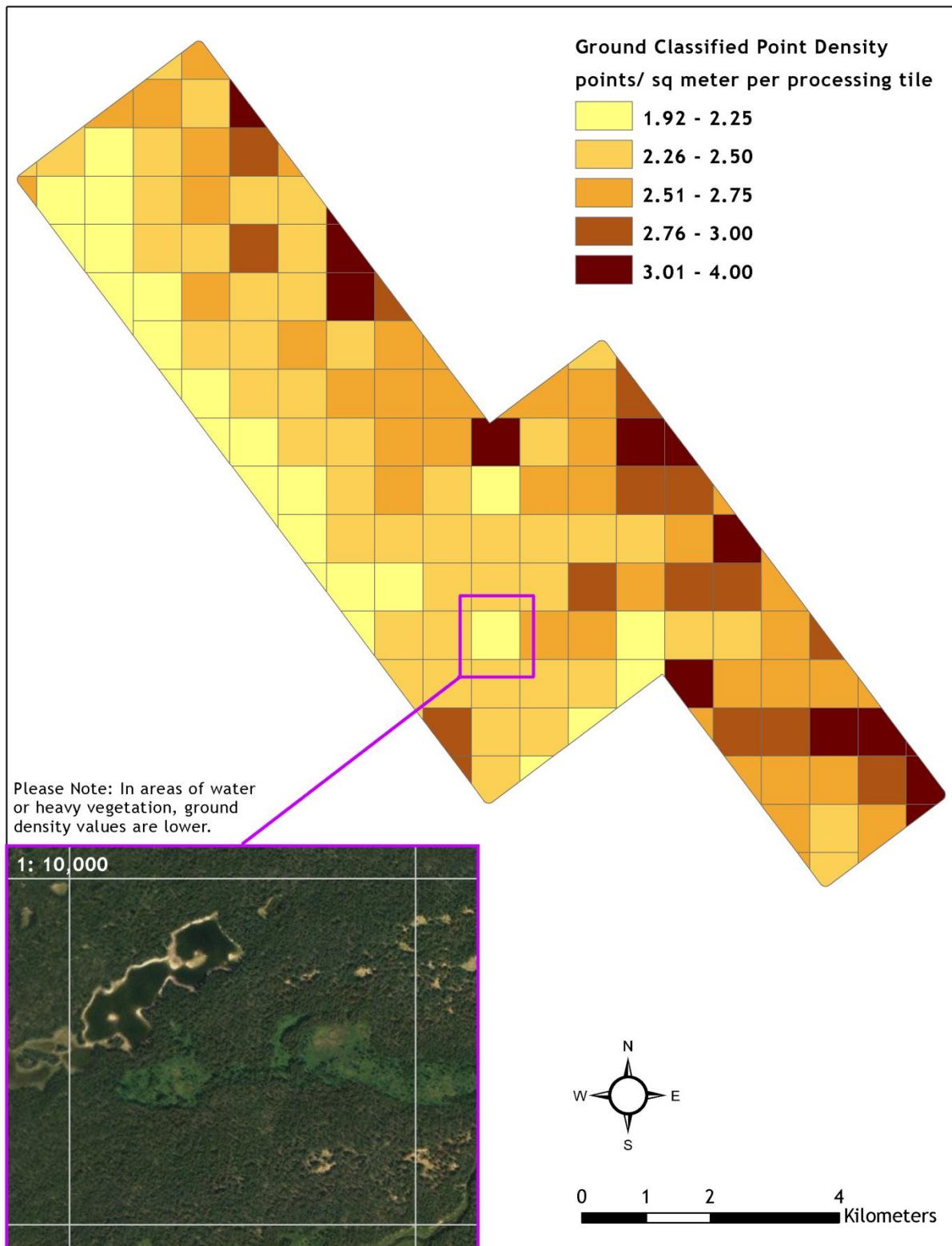


Figure 7. Density distribution map for ground return points by processing tile

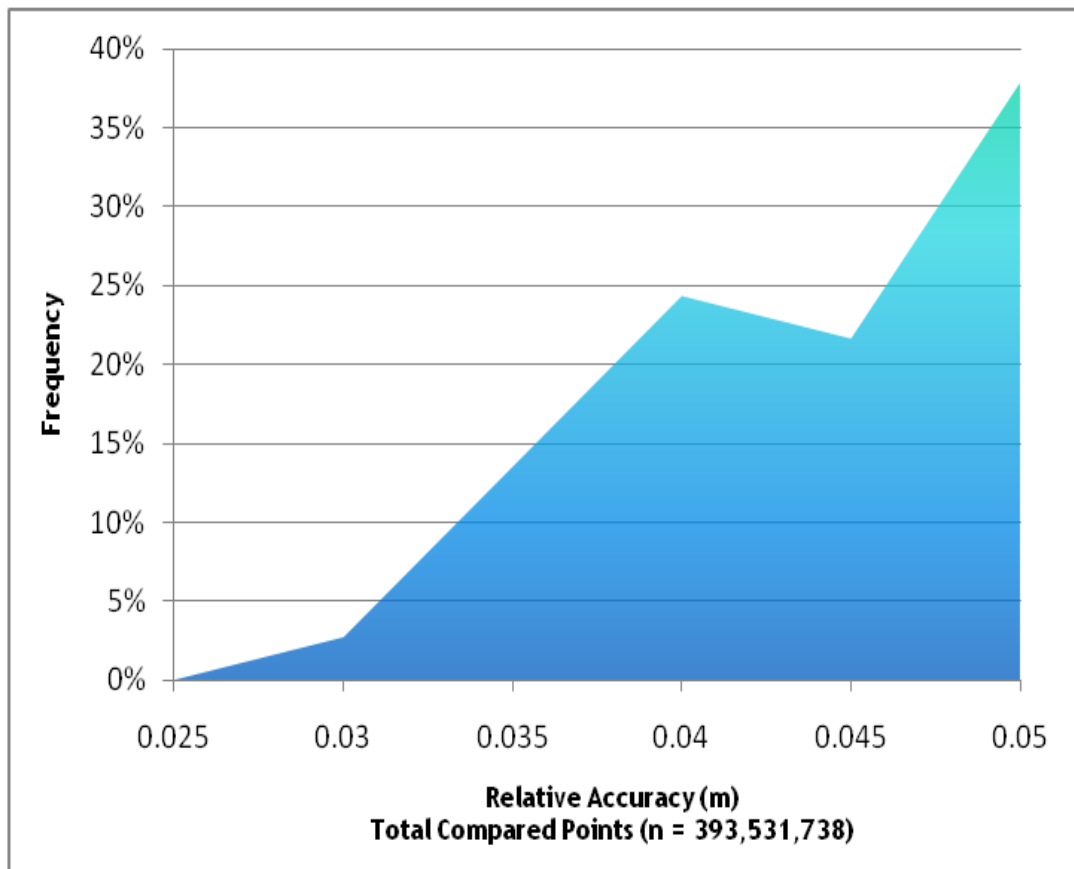


6.3 Relative Accuracy Calibration Results

Relative accuracy statistics for the Stanley dataset measure the full survey calibration including areas outside the delivered boundary:

- Project Average = 0.041 m
- Median Relative Accuracy = 0.043 m
- 1σ Relative Accuracy = 0.005 m
- 2σ Relative Accuracy = 0.011 m

Figure 8. Distribution of relative accuracies per flight line, non slope-adjusted



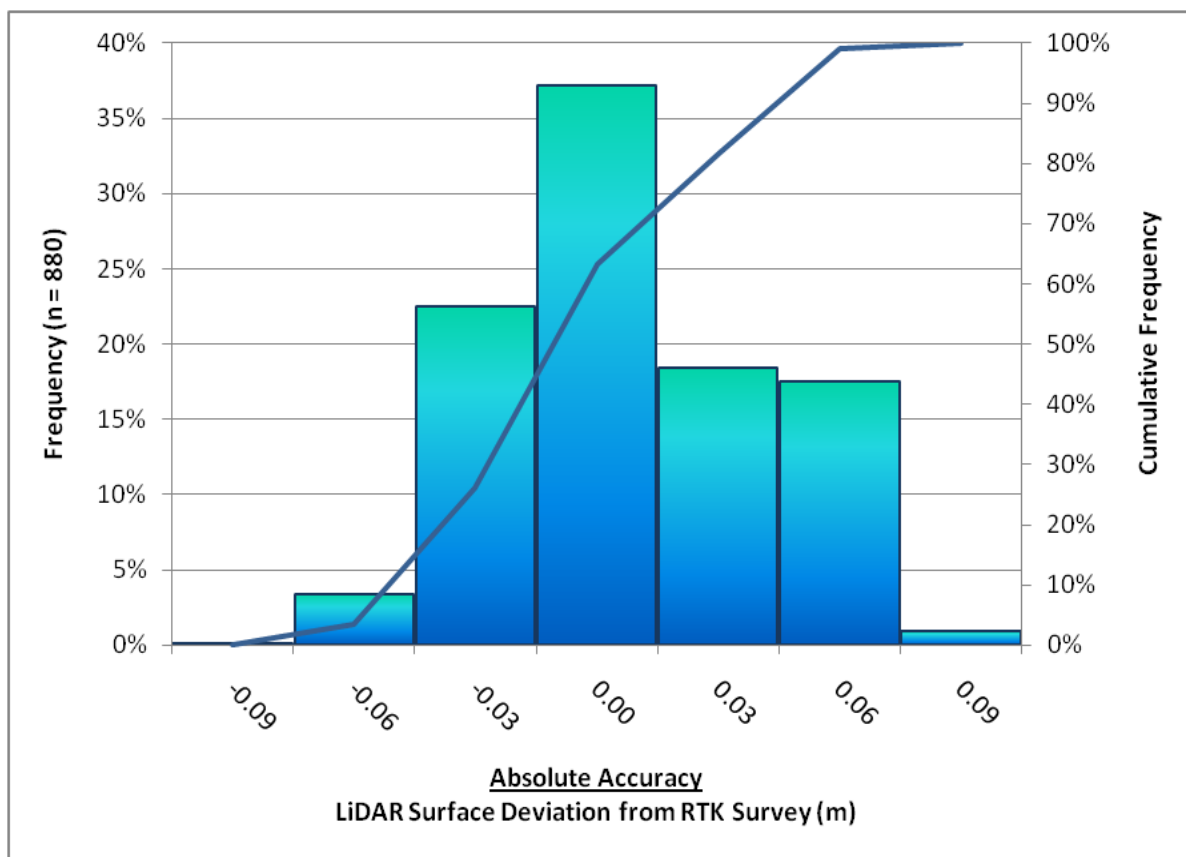
6.4 Absolute Accuracy

Absolute accuracies for the Stanley study area:

Table 2. Absolute Accuracy - Deviation between laser points and RTK hard surface survey points

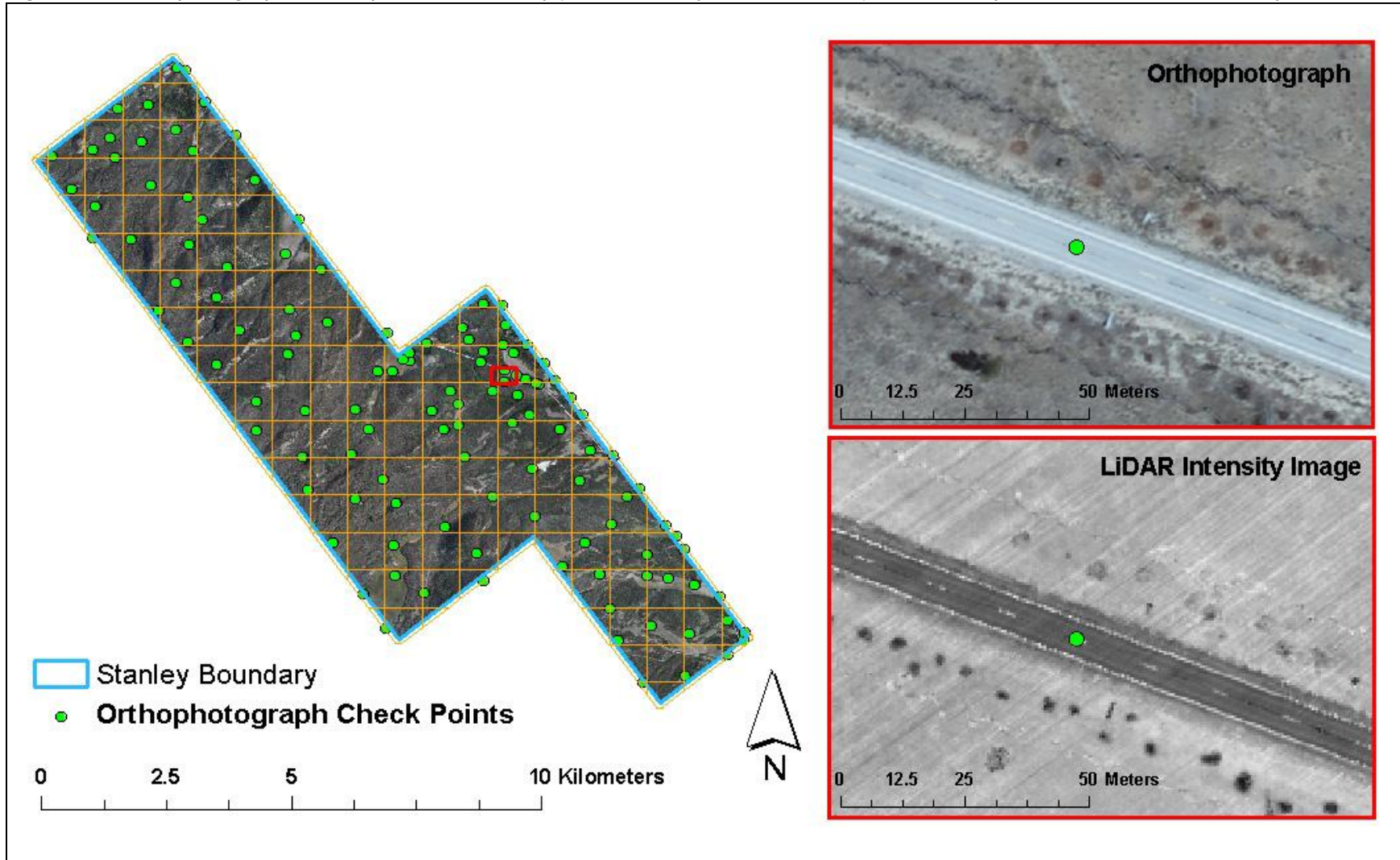
RTK Survey Sample Size (n): 880	
Root Mean Square Error (RMSE) = 0.033 m	Minimum Δz = -0.091 m
Standard Deviations 1 sigma (σ): 0.033 m 1.96 sigma (σ): 0.064 m	Maximum Δz = 0.071 m
	Average Δz = 0.007 m

Figure 9. Absolute Accuracy - Histogram Statistics, based on 880 RTK points



6.5 Orthophotograph Accuracy

Figure 10. Orthophotograph control point location map for the Stanley area. A total of 124 control points were used in this study.



For the survey area, 124 points were measured as horizontal and vertical references. These points, derived from the LiDAR intensity image, were used as control points for the aerial triangulation solution in LPS. The control points were collected/measured on features such as painted road-lines, soil features (e.g. wet spots), low lying shrubs, and boulders in the stream beds. The accuracy of the final aerial triangulation solution expressed as root mean square error (RMSE) was calculated in relation to the known control points.

Table 3. Triangulation and control point accuracy for photo processing 20 cm imagery.

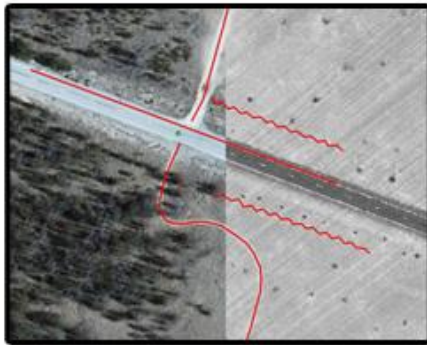
Total Image Unit-Weight RMSE¹: 1.81 pixel		
¹ Displays the total root mean square error for the triangulation. This standard deviation of unit weight is a global precision indicator describing the quality of the entire solution.		
Error measured as Control Point Residuals		
RMSE	X	Y
Control points	.65 m	.60 m

Additionally, a qualitative analysis was performed by visual inspection of the images against the LiDAR intensity images. This was to test the co-registration between the true-color images and the LiDAR data (**Figures 3 and 11**).

Figure 11. Example of visually inspecting co-registration of color images with LiDAR intensity image. The red lines were traced along painted road lines, fences, and down the center of two dirt roads in the LiDAR intensity image and then compared with the same locations in the ortho-rectified 4 Band image. Similar tests were performed on other features throughout the survey area.



**Features Traced on
LiDAR Intensity
Image
Scale 1:1000**



Visual Inspection



**Features Traced on
Orthophotograph
Scale 1:1000**

7. Projection/Datum and Units

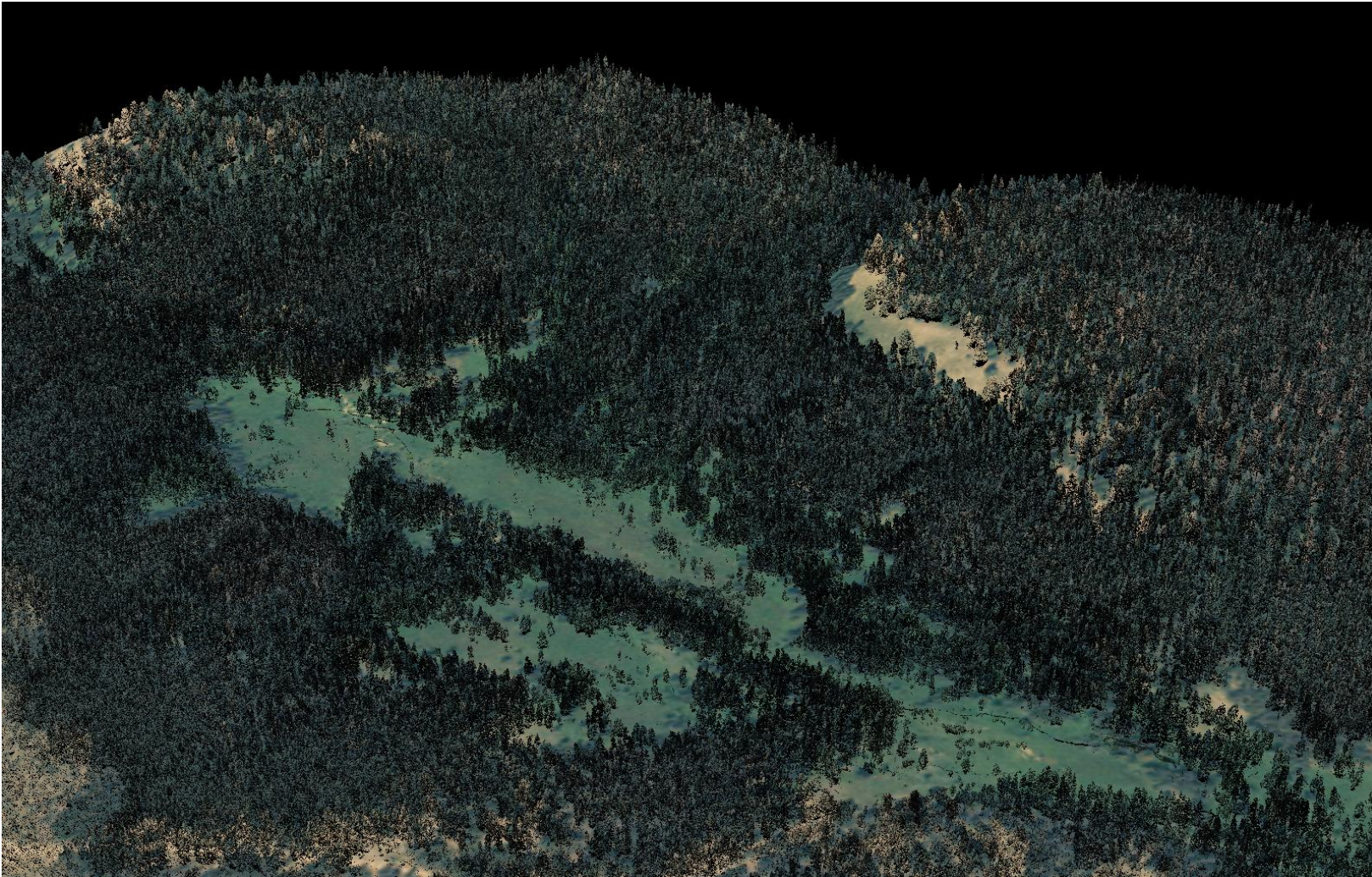
	Projection:	UTM Zone 11, NAD 83
Datum	Vertical:	NAVD88 Geoid03
	Horizontal:	NAD83
	Units:	meters

8. Deliverables

Point Data:	<ul style="list-style-type: none">• All Returns (LAS 1.2 format)
Vector Data:	<ul style="list-style-type: none">• Tile Index of LiDAR Points (shapefile format)
Raster Data	<ul style="list-style-type: none">• Elevation Models (1 m resolution)<ul style="list-style-type: none">• Bare Earth Model (ESRI GRID format)• Intensity images (GeoTIFF format, 0.5 m resolution)• Orthophoto 4-band tiles (GeoTIFF 16 bit format, 20 cm resolution)
Data Report:	<ul style="list-style-type: none">• Full report containing introduction, methodology, and accuracy

9. Selected Images

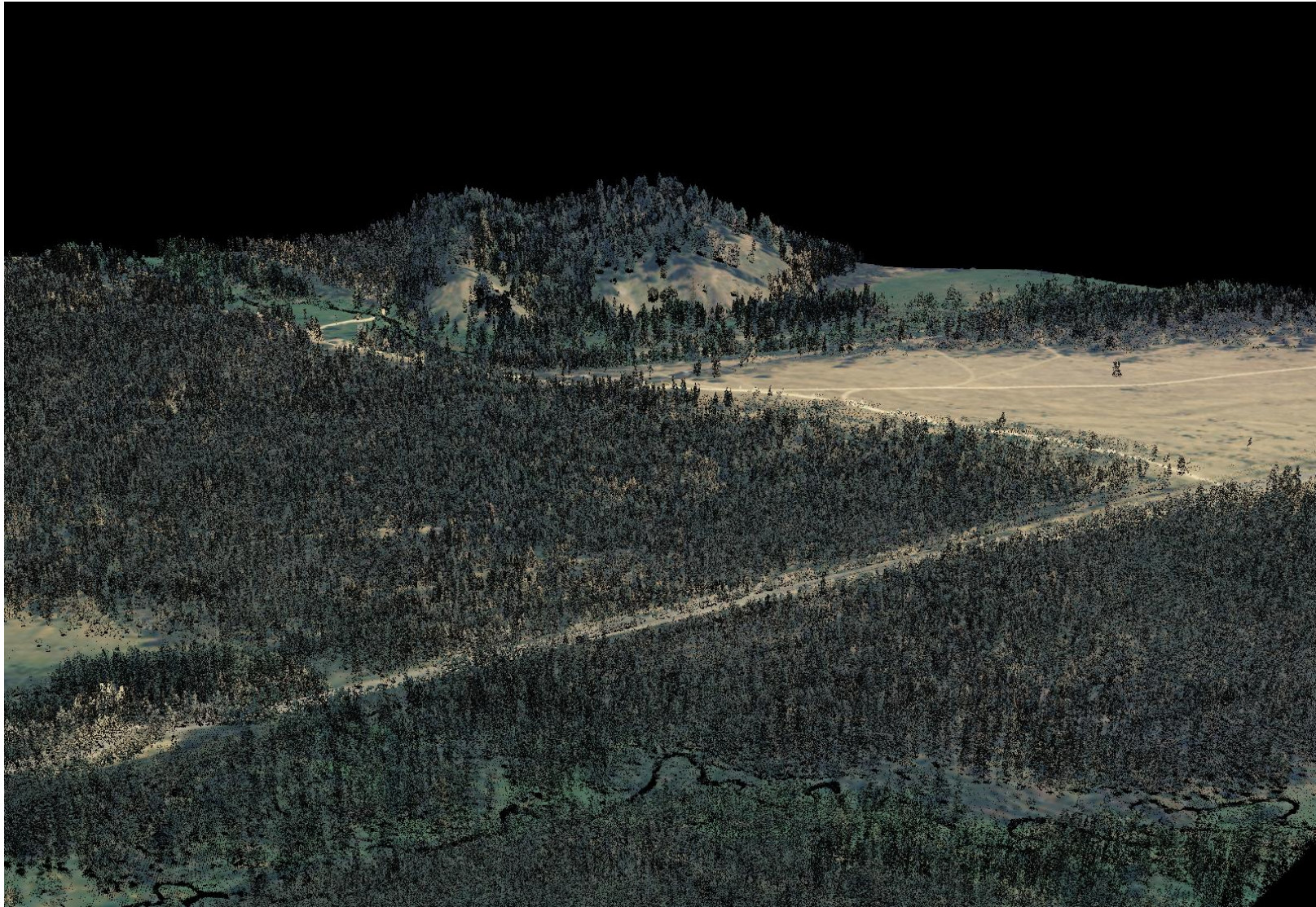
Figure 12. 3D LiDAR point cloud (with RGB values assigned) looking northwest at Thatcher Creek.



LiDAR Data Acquisition and Processing: Stanley, Idaho

Prepared by Watershed Sciences, Inc.

Figure 13. 3D LiDAR point cloud looking northeast at Meadow Creek running next to State Highway 21.



LiDAR Data Acquisition and Processing: Stanley, Idaho

Prepared by Watershed Sciences, Inc.

Figure 14. Bare Earth Model looking southeast at Meadow Creek.

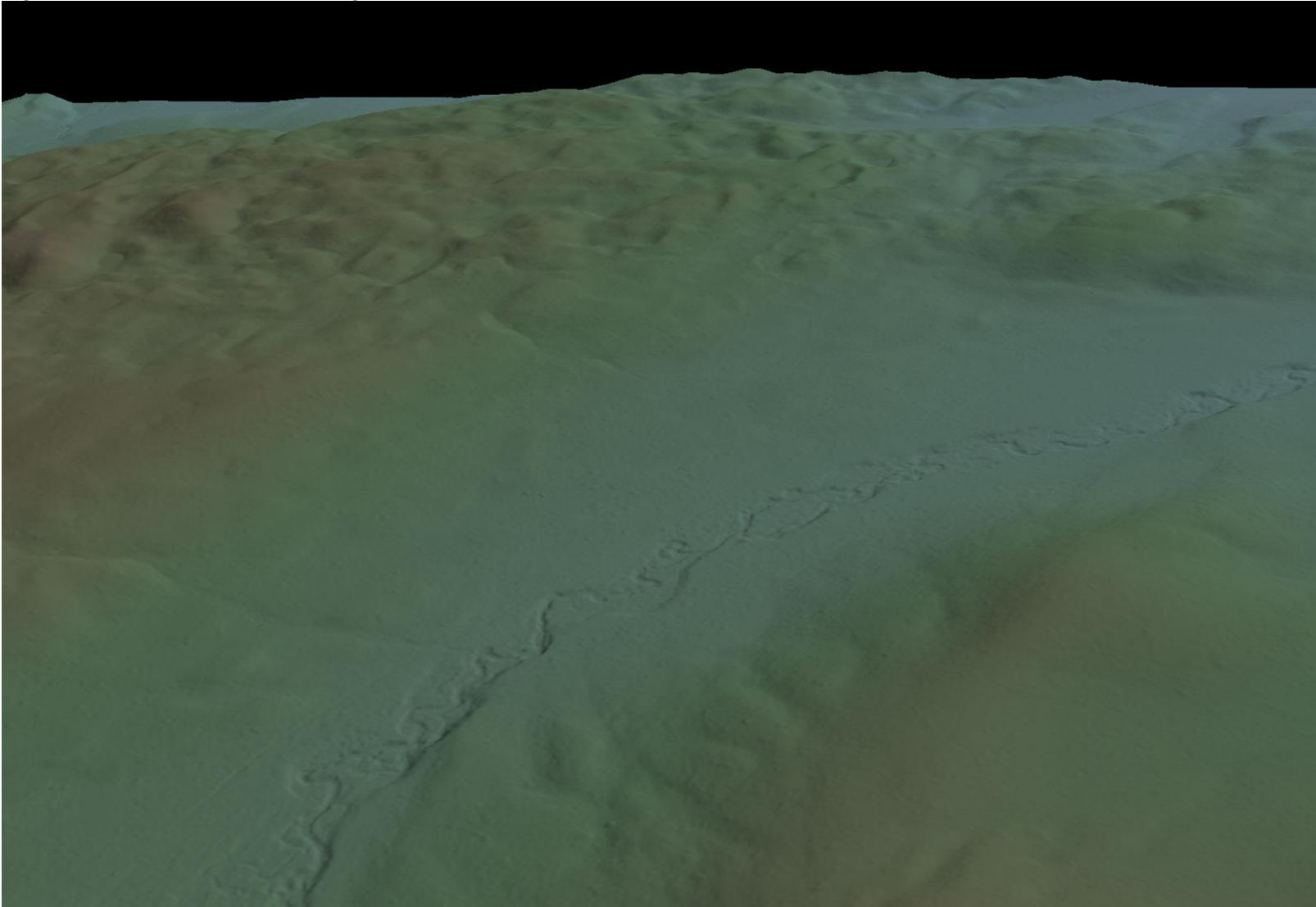


Figure 15. Bare Earth Model looking southeast at a distinctive terrai with several small lakes and Elk Creek in the background.

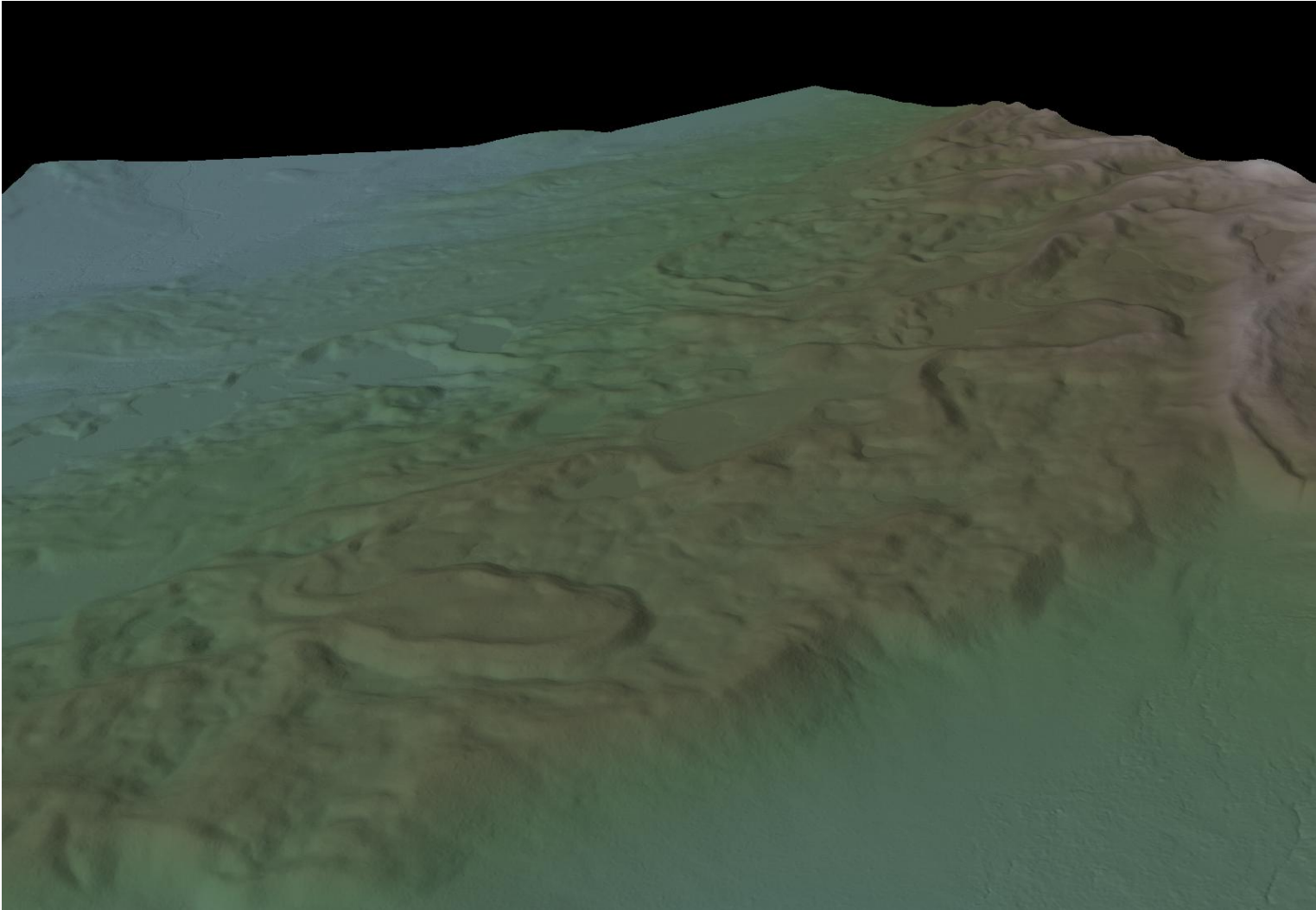
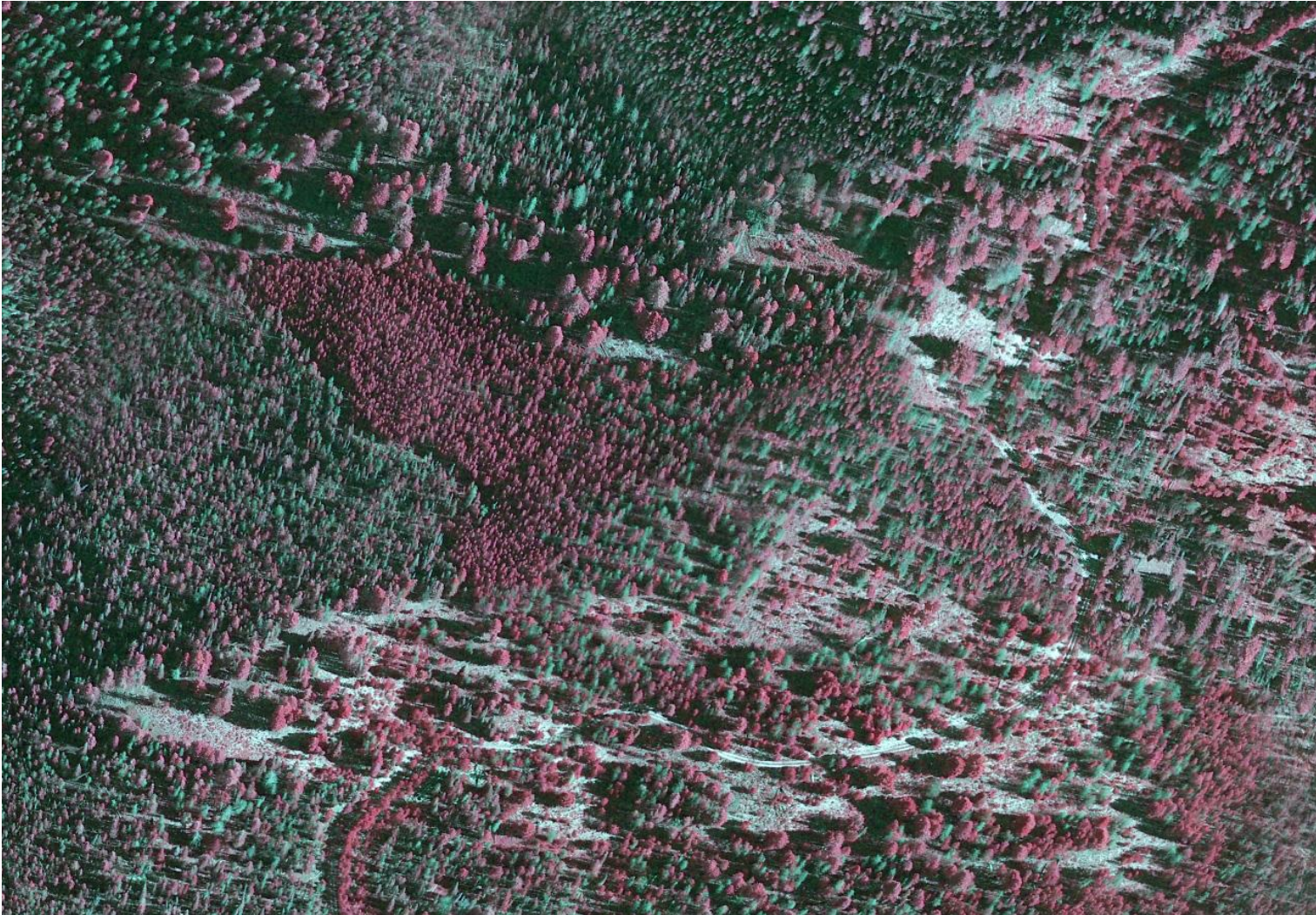


Figure 16. NIR image of two distinct stands within the Stanley study area.



10. Glossary

1-sigma (σ) Absolute Deviation: Value for which the data are within one standard deviation (approximately 68th percentile) of a normally distributed data set.

1.96-sigma (σ) Absolute Deviation: Value for which the data are within two standard deviations (approximately 95th percentile) of a normally distributed data set.

Root Mean Square Error (RMSE): A statistic used to approximate the difference between real-world points and the LiDAR points. It is calculated by squaring all the values, then taking the average of the squares and taking the square root of the average.

Pulse Rate (PR): The rate at which laser pulses are emitted from the sensor; typically measured as thousands of pulses per second (kHz).

Pulse Returns: For every laser pulse emitted, the Leica ALS 50 Phase II system can record *up to four* wave forms reflected back to the sensor. Portions of the wave form that return earliest are the highest element in multi-tiered surfaces such as vegetation. Portions of the wave form that return last are the lowest element in multi-tiered surfaces.

Accuracy: The statistical comparison between known (surveyed) points and laser points. Typically measured as the standard deviation (sigma, σ) and root mean square error (RMSE).

Intensity Values: The peak power ratio of the laser return to the emitted laser. It is a function of surface reflectivity.

Data Density: A common measure of LiDAR resolution, measured as points per square meter.

Spot Spacing: Also a measure of LiDAR resolution, measured as the average distance between laser points.

Nadir: A single point or locus of points on the surface of the earth directly below a sensor as it progresses along its flight line.

Scan Angle: The angle from nadir to the edge of the scan, measured in degrees. Laser point accuracy typically decreases as scan angles increase.

Overlap: The area shared between flight lines, typically measured in percents; 100% overlap is essential to ensure complete coverage and reduce laser shadows.

DTM / DEM: These often-interchanged terms refer to models made from laser points. The digital elevation model (DEM) refers to all surfaces, including bare ground and vegetation, while the digital terrain model (DTM) refers only to those points classified as ground.

Real-Time Kinematic (RTK) Survey: GPS surveying is conducted with a GPS base station deployed over a known monument with a radio connection to a GPS rover. Both the base station and rover receive differential GPS data and the baseline correction is solved between the two. This type of ground survey is accurate to 1.5 cm or less.

10. Citations

Soininen, A. 2004. TerraScan User's Guide. TerraSolid.

Appendix A

LiDAR accuracy error sources and solutions:

Type of Error	Source	Post Processing Solution
GPS (Static/Kinematic)	Long Base Lines	None
	Poor Satellite Constellation	None
	Poor Antenna Visibility	Reduce Visibility Mask
Relative Accuracy	Poor System Calibration	Recalibrate IMU and sensor offsets/settings
	Inaccurate System	None
Laser Noise	Poor Laser Timing	None
	Poor Laser Reception	None
	Poor Laser Power	None
	Irregular Laser Shape	None

Operational measures taken to improve relative accuracy:

1. Low Flight Altitude: Terrain following is employed to maintain a constant above ground level (AGL). Laser horizontal errors are a function of flight altitude above ground (i.e., $\sim 1/3000^{\text{th}}$ AGL flight altitude).
2. Focus Laser Power at narrow beam footprint: A laser return must be received by the system above a power threshold to accurately record a measurement. The strength of the laser return is a function of laser emission power, laser footprint, flight altitude and the reflectivity of the target. While surface reflectivity cannot be controlled, laser power can be increased and low flight altitudes can be maintained.
3. Reduced Scan Angle: Edge-of-scan data can become inaccurate. The scan angle was reduced to a maximum of $\pm 15^\circ$ from nadir, creating a narrow swath width and greatly reducing laser shadows from trees and buildings.
4. Quality GPS: Flights took place during optimal GPS conditions (e.g., 6 or more satellites and PDOP [Position Dilution of Precision] less than 3.0). Before each flight, the PDOP was determined for the survey day. During all flight times, a dual frequency DGPS base station recording at 1-second epochs was utilized and a maximum baseline length between the aircraft and the control points was less than 19 km (11.5 miles) at all times.
5. Ground Survey: Ground survey point accuracy (i.e. <1.5 cm RMSE) occurs during optimal PDOP ranges and targets a minimal baseline distance of 4 miles between GPS rover and base. Robust statistics are, in part, a function of sample size (n) and distribution. Ground survey RTK points are distributed to the extent possible throughout multiple flight lines and across the survey area.
6. 50% Side-Lap (100% Overlap): Overlapping areas are optimized for relative accuracy testing. Laser shadowing is minimized to help increase target acquisition from multiple scan angles. Ideally, with a 50% side-lap, the most nadir portion of one flight line coincides with the edge (least nadir) portion of overlapping flight lines. A minimum of 50% side-lap with terrain-followed acquisition prevents data gaps.
7. Opposing Flight Lines: All overlapping flight lines are opposing. Pitch, roll and heading errors are amplified by a factor of two relative to the adjacent flight line(s), making misalignments easier to detect and resolve.

